WARSAW UNIVERSITY OF TECHNOLOGY Index 351733
FACULTY OF CIVIL ENGINEERING
COMMITTEE FOR CIVIL AND WATER ENGINEERING
POLISH ACADEMY OF SCIENCES ISSN 1230-2945
DOI: 10.24425/ace.2025.153323
ARCHIVES OF CIVIL ENGINEERING
Vol. LXXI ISSUE 1 2025
pp. 99–112

Research paper

Stress loading effect research of plastic damage materials based on D-SAP and finite element analysis

Xiaofeng Liu[1], Yanli Wang[2], Chengyuan Lu[3]

Abstract: This study mainly analyzes the stress loading effect of current plastic damaged materials and investigates the stress changes during plastic material damage. The stress structure of the material is analyzed using D-SAP software and the finite element analysis. A new analysis system for plastic damage materials is established. The new system can analyze the damage stress and rigidity magnitude of plastic materials. These studies confirm that new system software can to some extent complete the analysis of stress loading effects on plastic damaged materials. The simulation curve of the software is basically consistent with the experimental values. When compared with traditional software for testing, the new software shows significantly better performance in simulating stress situations and accuracy compared to traditional analysis and simulation software. D-SAP and Digimat software show different deviations during testing. D-SAP has the smallest stress variation, while Digimat strain and stress testing has a larger deviation. In the stiffness test, the deviation between the two software is between 2.04% and 5.3%. In multi-axis pressure testing, D-SAP is consistent with the test values. Therefore, the software used in this study has a better effect on analyzing the stress loading effect of the material, and the deviation between the tested stress and stiffness is smaller. This provides a new direction for stress analysis of materials.

Keywords: D-SAP, finite element, loading effect, plastic damage, stress

[1]Assoc Prof., School of CML Engineering Architecture, Zhejiang Guangsha Vocational and Technical University of Construction, Dongyang, 322100, China, e-mail: 13566925372@163.com, ORCID: 0009-0002-5584-1555
[2]Eng., Department of Technology Development, Dongyang Third Construction Engineering Co., Ltd, Zhejiang Dongyang, 322100, China, e-mail: wangyanli2023001@126.com, ORCID: 0009-0007-8441-1382
[3]Prof., College of Civil Engineering, Zhejiang University of Technology, Hangzhou, 310000, China, e-mail: luchengyuan2023@163.com, ORCID: 0009-0002-2343-279X

1. Introduction

Accurate Stress Analysis (SA) of plastic damaged materials is essential in modern engineering and materials science [1]. SA not only helps to understand the behavior of materials under different conditions, but is also crucial for designing more reliable and durable structural components [2]. With the rapid development of computing technology, various simulation methods of computers have become important tools for studying material stress [3]. Fine Element Analysis (FEA), as a commonly used computer analysis method, has been widely applied in stress and strain analysis of various materials. D-SAP, as an advanced analytical tool, has shown excellent performance in simulating complex material behavior, especially in material stress response under multi axial pressure conditions [4]. But at the same time D-SAP software in the analysis of plastic materials in the analysis of the material stress analysis is more complex can not be an accurate model of the individual material nodes, followed by the software's parametric analysis of the less efficient to build the model is less efficient. Therefore, the study hopes to achieve the modeling and analysis of the material structure by building a material parametric analysis model using D-SAP software. Based on this, this study combines D-SAP with traditional FEA to build a more comprehensive analysis and simulation software to analyze the stress changes of plastic damage materials under different loading conditions. To improve the SA effect, the stress changes and rigid section parameters of the material are analyzed in this software. Using the stiffness matrix in the software, the stress changes in the model are calculated to ensure that the structural characteristics and parameter changes of plastic materials can be analyzed correctly. At the same time, the introduction of finite elements enhances the accuracy of the software's testing of materials and improves the effectiveness of stress testing. Through the plastic damage material stress analysis, can enhance the understanding of the current plastic material analysis, the weak part of the strengthening, so as to enhance the understanding of the degree of material, at the same time on the construction of the collapse of the material failure and other issues to play a better role in guiding. This study consists of four parts in total. Firstly, it is an overview of domestic and international research. Secondly, the software system is built. Next, the testing effectiveness of this software is analyzed. Finally, there is a summary of this article.

2. Related works

The use of materials and damage analysis in engineering analysis are important steps in current construction projects. Many experts and scholars have analyzed the stress and plastic damage of materials in this direction. Zhou et al. used a combination of numerical simulation and experimental analysis to study the thermal stress distribution of PCM glass units. The new method could analyze the heat transfer performance and thermal stress distribution of PCM glass units with a thickness between 3 and 11 millimeters. These results indicated that the addition of PCM improved the thermal performance of glass units. Among these five testing facilities, the glass unit surface with a PCM layer thickness of 7 millimeters showed the smallest thermal strain change [5]. Aurichio et al. proposed an optimization scheme based on phase

field method to solve the structural topology optimization problem in 3D printing process. This method considered factors such as stress constraints and multiple materials or scales. These results indicated that this method had high sensitivity to parameters. Finally, the feasible workflow from numerical solutions to 3D printing objects was analyzed, and the final structure of these results was completed using melt deposition modeling of 3D printers [6]. Kumar et al. established a three-dimensional finite element model of implanted pelvic bone using CT data. They investigated the effects of interface cracks and implant materials on mixed mode stress intensity factors, as well as predicting interface failure of bone cement acetabular cups. And a two-dimensional crack model was developed and solved using the element free Galerkin method. These results indicated that the stress intensity factor in the front was higher and might be more prone to failure. Compared with the interface of bone cement, the stress intensity factor of ceramic ceramic material combination was lower [7]. Oyeniran et al. conducted a numerical analysis using the FEA tool ABAQUS software to investigate the effect of residual stress on fatigue damage of single piles in offshore wind turbines. Three single-pile models with the same size were developed in ABAQUS, and characteristic loads were applied to all models. These results indicated that the maximum impact of tensile residual stress on fatigue damage of single piles was 0.05%, while the impact of compressive residual stress on fatigue life of single piles was 0.06%. The influence of residual stress on stress accumulation in the critical welding zone could be ignored [8].

Chen et al. used the coupled stress elasticity method to study the "anti-plane shear cracks" at the interface of bonded heterogeneous elastic media with initial stress. The new method proved the deviation of the coupled stress tensor and derives the governing equation of the relevant boundary conditions. And it used the feature function expansion method to determine the singularity index. These results indicated that the inherent characteristic length, coupled stress material constant, and initial stress had a significant impact on crack tearing displacement, coupled stress intensity factor, and energy release rate [9]. Siqueira et al. proposed a new constitutive model based on fluidity to study the rheological properties of thixotropic yield stress materials in cylindrical Couette fluids. The new model coupled the motion equation with the additional equation of material fluidity evolution, and fluidity was used as a structural parameter without the need to introduce phenomenon functions or additional parameters. These results indicated that the fracture and stacking process of microstructure, as well as the position of the yield surface in flow, depended on the applied stress and the characteristics of these two materials. In addition, steady-state flow was solely determined by the applied stress and did not depend on the initial structural state of the material [10]. Chen et al. proposed a new local stress-strain estimation method to investigate the low cycle fatigue characteristics of cold drawn steel under strain controlled uniaxial fatigue loading. The experimental results indicated that, except for the initial period of cyclic hardening, cyclic softening phenomenon could be observed throughout the entire fatigue life. And the new method was more accurate than traditional methods, and the maximum relative error between predicting fatigue life and experimental fatigue life was less than 6% [11]. Li et al. proposed a new fatigue crack growth model to address the fatigue of crack like defects in engineering structures under variable amplitude loading conditions. The new model was based on the energy principle during crack growth and included an equivalent factor N that was independent of the material. It theoretically

explained the effect of stress ratio on the FCG rate of metal materials. These results indicated that the new model provided a more accurate relationship between stress ratios and FCG rates of various metal materials. This provided an effective strategy for predicting the fatigue life of cracked components under variable amplitude loading [12].

In summary, in current research, some software and theoretical models are mainly used to analyze and detect the SA of materials. Therefore, this study analyzes and simulates the stress of plastic damage materials and builds a new model combining D-SAP and finite element to analyze and study the stress and rigidity of materials. Through different analysis methods of the two models, judgment and effect analysis are made from different stress situations of materials. This further enhances the SA effect of the current model on materials. The analytical accuracy and applicability of traditional methods are limited by simplified models that cannot accurately predict material conditions under complex loads or geometries. In contrast, the new modeling approach combining D-SAP and finite elements provides a deeper understanding of the material failure process by taking into account the interaction of material damage and plastic flow, and is suitable for analyzing the behavior of high-performance materials under extreme conditions.

3. Effect research of plastic damage materials based on D-SAP and finite element unit

This chapter mainly analyzes and studies D-SAP and finite element theory and builds a new system material analysis model. By analyzing the different parameters of materials, the current research system model is improved. Finally, a material testing system platform is built on the basis of this model.

3.1. D-SAP and finite element analysis module construction

D-SAP programs generally encode the current object using C++ encoding. It mainly analyzes the language and attribute characteristics of the research objects, so the demand for standardization is relatively high. FEA is a computational tool used to predict how an object reacts to external factors such as force, heat, vibration, pressure, etc. [13]. It simulates the physical behavior of an object by dividing a complex entity or system into multiple small, simple, and interconnected units. Therefore, adding finite element units to D-SAP can achieve performance analysis of current material parameters and other properties. Fig. 1 shows the overall structure of the analysis model.

In Fig. 1, the overall analysis structure of the studied model includes four modules: D-SAP framework, interface module, core algorithm analysis, and material unit. The program interface module is mainly responsible for receiving information parameters of this program. The core algorithm module mainly uses some algorithm models and finite element elements to analyze parameters. The material unit module is mainly used for in-depth analysis and research of materials that need to be analyzed. Finally, the analysis and simulation of building structures and materials are completed through the combination of four modules.

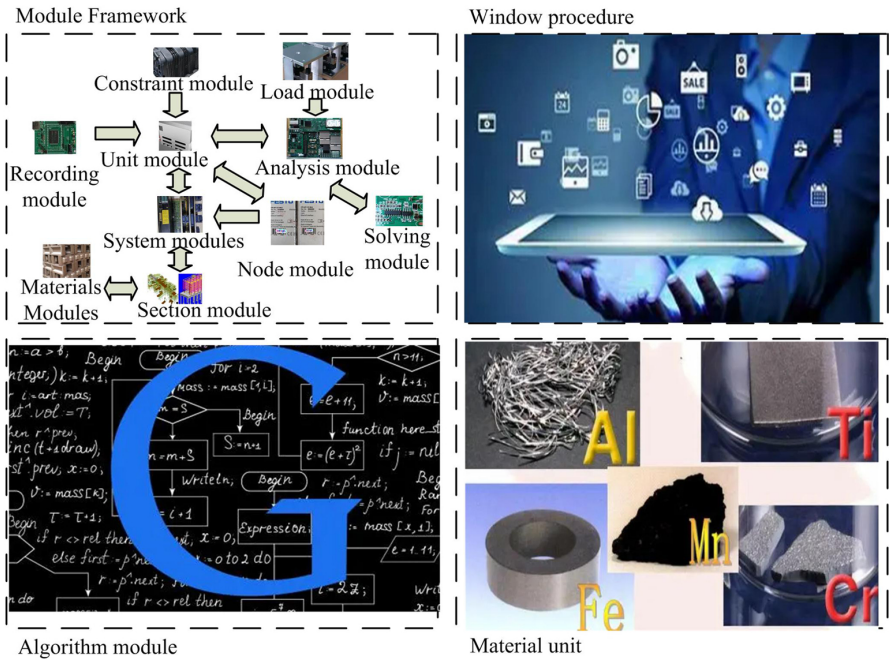

Fig. 1. D-SAP software program analysis model structure

3.2. Stress analysis of plastic damage materials based on D-SAP program and finite element unit

In general engineering, due to the large size and complex shape of the structural units encountered, it is necessary to convert the unit structure of lotus picking during the solving process. Therefore, an equal parameter conversion method is used, such as the parameter coordinate unit conversion formula in Eq. (3.1) [14].

$$\begin{Bmatrix} x \\ y \\ z \end{Bmatrix} = f \begin{Bmatrix} L_1 \\ L_2 \\ L_3 \\ L_4 \end{Bmatrix} \tag{3.1}$$

In Eq. (3.1), L_1 represents the volume coordinates of the material unit at position 1, L_2 represents the volume coordinates of the material unit at position 2, L_3 represents the volume coordinates of the material unit at position 3, and L_4 represents the volume coordinates of the material unit at position 4. Taking tetrahedral materials as an example, interpolating the coordinates yields Eq. (3.2).

$$x = \sum_{i=1}^{m} N_i' x_i, \quad y = \sum_{i=1}^{m} N_i' y_i, \quad z = \sum_{i=1}^{m} N_i' z_i \tag{3.2}$$

In Eq. (3.2), m represents the number of unit nodes. x_i represents the horizontal coordinates of the node, y_i represents the vertical coordinates of the node, and z_i represents the vertical coordinates of the node. $N_i^{'}$ represents the size of the coordinate interpolation function for the node [15]. Interpolation functions can analyze materials in different states and shapes at present. Simultaneously using stiffness matrices can achieve generalized format analysis of material problems. Fig. 2 is a schematic diagram of the stiffness matrix process.

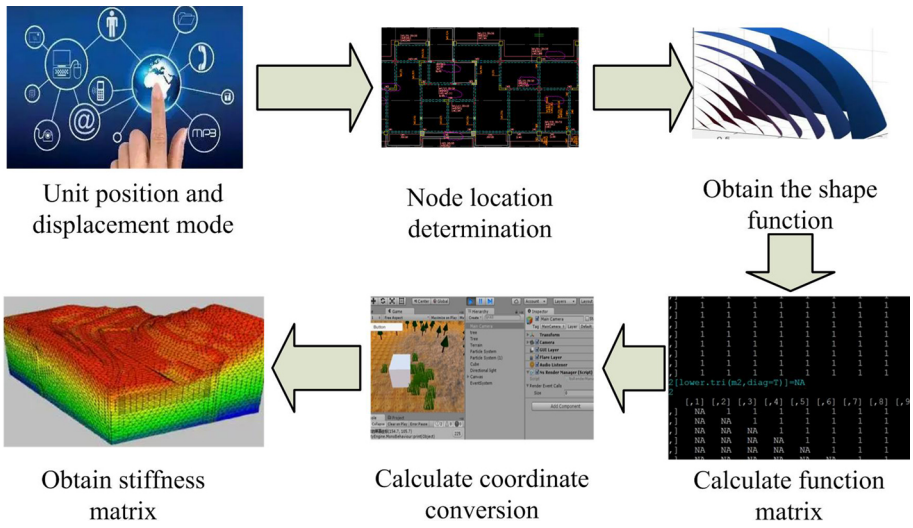

Fig. 2. Rigidity matrix process

In Fig. 2, when confirming the element stiffness of the material, first determine the unit position and displacement mode, need to determine the unit position information and displacement mode, using finite element to calculate the node position of the material, through the interpolation function to obtain the shape function. Secondly, calculate the node position and shape function, when the displacement of the unit is clearer, the more accurate material parameter information is obtained, and then solve the coordinate information parameters, through the function to solve the total coordinate information parameters to get the matrix H. And then carry out the coordinate conversion and derivation, because the coordinates of the function belong to the interpolation coordinates, so through the derivation of the total coordinates can be completed to transform the coordinates of the matrix. After that, the potential energy is solved and the stiffness matrix expression is obtained by solving the potential energy to get the expression of the stiffness matrix, and finally the unit stiffness matrix is solved by integrating, and the unit stiffness matrix is obtained by choosing the appropriate value of the stiffness matrix to be integrated and solved. The stiffness matrix is mainly used to solve the problems of two-dimensional line surface coordinates of current materials. For the three-dimensional damage degree and SA of damaged materials, it is necessary to build a model in Eq. (3.3).

$$\sigma = (1 - w_t)\overline{\sigma}_t + (1 + w_c)\overline{\sigma}_c \tag{3.3}$$

In Eq. (3.3), $\overline{\sigma}_t$ represents the effective tensor for bearing tensile stress, $\overline{\sigma}_c$ represents the effective tensor for bearing compressive stress, σ represents the stress tensor, w_t represents the damage variable for pressure, and w_c represents the damage variable for tension. The effective stress tensor can be obtained from Eq. (3.4) [16].

$$\overline{\sigma} = D_c : (\tau - \tau_p) \tag{3.4}$$

In Eq. (3.4), $\overline{\sigma}$ is the magnitude of effective stress. D_c represents the elastic stiffness matrix. τ represents the total strain magnitude value, and τ_p represents the plastic strain magnitude value, respectively. The plasticity expression of damaged materials can be expressed as a function in Eq. (3.5).

$$f_p(\overline{\sigma}, \kappa_p) = F(\overline{\sigma}, q_{h1}, q_{h2}) \tag{3.5}$$

In Eq. (3.5), κ_p represents the magnitude of plastic hardening. q_{h1} represents the hardening function size of the material surface, and q_{h2} represents the hardening function size of the size, respectively. The flow rule at this time is represented by Eq. (3.6) [17].

$$\overline{\varsigma}_p = \overline{\lambda}\frac{\partial g_p}{\partial \overline{\sigma}}(\overline{\sigma}, \kappa_p) \tag{3.6}$$

In Eq. (3.6), $\overline{\varsigma}_p$ represents the rate of change in plastic strain rate. $\overline{\lambda}$ is the liquidity factor. g_p represents the potential energy function. The tension effect on the loading and unloading of the model is represented by Eq. (3.7).

$$\begin{aligned} f_{dt} &= \overline{\varepsilon}_t(\overline{\sigma}) - \kappa_p \\ \omega_t &= g_{dt}(\kappa_{dt}, \kappa_{dt1}, \kappa_{dt2}) \end{aligned} \tag{3.7}$$

In Eq. (3.7), f_{dt} represents the size of the loading function. $\overline{\varepsilon}_t(\overline{\sigma})$ means stress changes with the same effect. κ_{dt}. κ_{dt1} and κ_{dt2} all represent the historical variable size of material damage. The pressure effect at this time is represented by Eq. (3.8).

$$\begin{aligned} f_{dc} &= a_c\overline{\varepsilon}_c(\overline{\sigma}) - \kappa_{dc} \\ \omega_c &= g_{dc}(\kappa_{dc}, \kappa_{dc1}, \kappa_{dc2}) \end{aligned} \tag{3.8}$$

In Eq. (3.8), a_c represents the change in stress state under pressure, while the other parameters undergo the same changes as mentioned above. The yield function in plasticity is represented by Eq. (3.9) [18].

$$\overline{\sigma}_v = \frac{I_1}{3}, \quad \overline{p} = \sqrt{2J_2}, \quad \overline{\theta} = \frac{1}{3}\arccos\left(\frac{3\sqrt{3}}{2}\frac{J_3}{J_2^{3\sqrt{2}}2}\right) \tag{3.9}$$

In Eq. (3.9), $\overline{\sigma}_v$ is the strain force change of the effective material volume. $\overline{p}$ represents the coordinate size of the second position of the material column. $\overline{\theta}$ represents the size of the Lode angle. I_1 represents the first tensor of stress, J_2 represents the second invariant of stress, and J_3

represents the third invariant of stress. The variable variation of the yield function can control the shape and size of the material, and the hardening rule is represented by Eq. (3.10).

$$q_{h1}(\kappa_p) = \begin{cases} q_{h0} + (1 - q_{h0})(\kappa_p^3 - 3\kappa_p^2 + 3\kappa_p) - H_p(\kappa_p^3 - 3\kappa_p^2 + 2\kappa_p), & \kappa_p < 1 \\ 1, & \kappa_p \geq 1 \end{cases} \tag{3.10}$$

In Eq. (3.10), H_p represents the slope. q_{h1} represents the shape hardening function, and the other parameters are the same as above. The size hardening function is represented by Eq. (3.11).

$$q_{h2} = \begin{cases} 1, & \kappa_p < 1 \\ 1 + H_p(\kappa_p - 1), & \kappa_p < 1 \end{cases} \tag{3.11}$$

The parameters in Eq. (3.11) are the same as above. Under normal circumstances, one-dimensional plastic damage can be expressed by Eq. (3.12) as the relationship between strain and stress changes.

$$\sigma = (1 - \omega)\overline{\sigma} = (1 - \omega)E(\varepsilon - \varepsilon_p) \tag{3.12}$$

In Eq. (3.12), ω means the change in the degree of damage under tension and pressure. ε is the total strain force magnitude. ε_p represents the magnitude of plastic strain force. The damage variable of materials can be solved through iterative algorithms, represented by Eq. (3.13) [19].

$$(1 - \omega)E\kappa_{dc} - f_t \exp\left(-\frac{\kappa_{dc1} + \omega\kappa_{dc2}}{\varepsilon_{fc}}\right) = 0, \varepsilon > 0 \tag{3.13}$$

The parameters in Eq. (3.13) are the same as the above formulas. A new model vector has been summarized through the analysis of material stress.

3.3. System model construction for plastic damage material analysis based on D-SAP program and finite element unit

To ensure stable analysis of material damage in D-SAP, parameter calculations need to be performed using the above equations, and the material parameters need to be converted into formula code and input into the program. The main encoding of D-SAP is programmed through C++. Therefore, the program utilizes the characteristics of C++ to perform damage calculations on materials, such as unit algorithms in Fig. 3.

In Fig. 3, when conducting damage calculations in D-SAP, it is necessary to first calculate the equivalent strain size of the material, and then calculate the equivalent tensile strain force and equivalent compressive strain force of the material. The incremental strain force of material plasticity was obtained through the damage function, and the ductility coefficient of the material was calculated. Afterwards, it is determined whether the current tensile damage function is greater than 0. If it is greater than 0, the historical tensile and compressive variables of the material are calculated, and then the damage variable is calculated to determine the compressive damage function. If it is less than 0, the compression damage function is judged directly. If

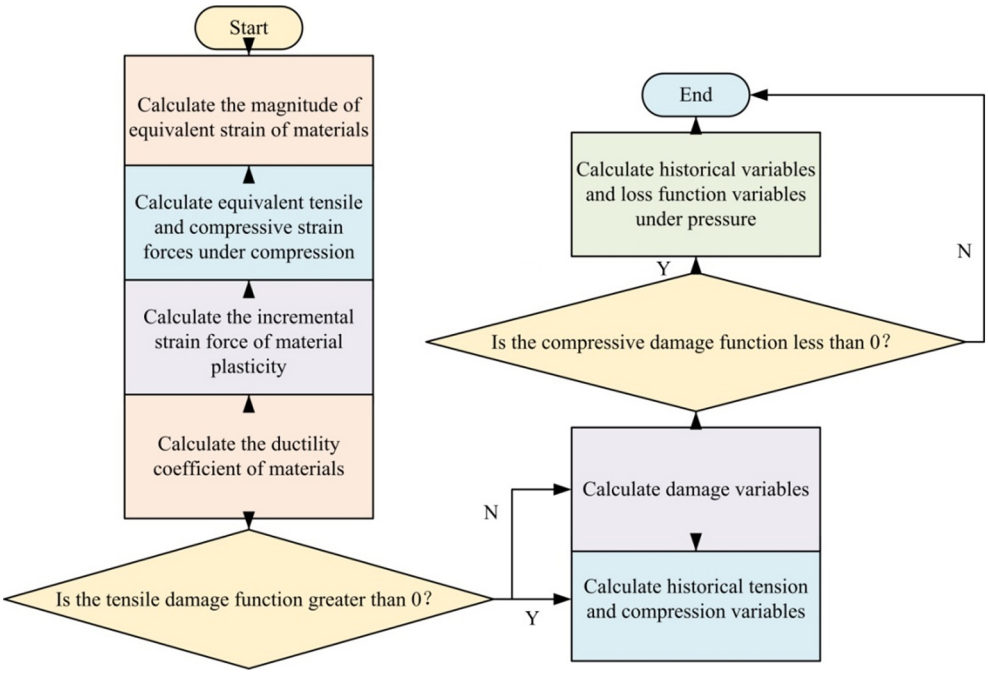

Fig. 3. Material damage calculation process

the compression damage function is greater than 0, the historical variables and loss function variables of compression are calculated. If it is less than 0, the process is terminated directly.

Most methods only analyze the process of strain, which is less considered for subsequent updates and changes in damage values [20]. Therefore, a method for calculating Patix damage parameters is added throughout the entire D-SAP. When the slope of the damage change curve of plastic materials is small, the damage value of the material is reduced during unloading and loading to alleviate the reduction of material stress and stiffness when the material undergoes stiffness and stress direction changes. And the damage of the material is reduced according to the magnitude of stress and stiffness to deal with the stress change and stiffness mismatch [21].

4. Stress loading effect analysis of plastic damaged materials based on D-SAP and finite element analysis

To verify the importance and situation change analysis of the current D-SAP software in material damage SA, polystyrene was selected as the research example material for analysis. The parameter values of the selected material were $E = 26$ GPa, $v = 0.2$, $f_c = 35$ MPa, and $f_t = 3.5$ MPa. The finite element in the model test is a four-node finite element. The model consists of 100 four-node finite element elements with a total number of nodes of 400. In

the four-node finite element, the displacement field is defined by the displacements at the nodes defined by interpolating throughout the element using a shape function that includes the displacements in the X and Y directions along the element boundaries. The stress field is calculated from the derivatives of the displacement field as well as the intrinsic relationship of the material. Fig. 4 is a schematic diagram of the compression and tension situations, actual value represent data values obtained from actual stress compression experiments, and D-SAP data values represent data values calculated by the D-SAP program software.

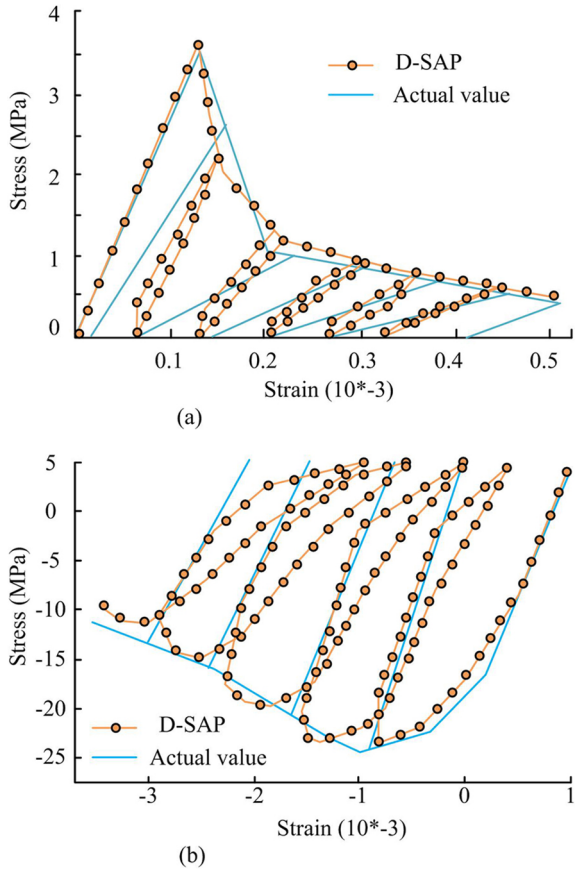

Fig. 4. Stress variation of damaged materials under compression and tension: (a) The stress change of materials affected by tensile force, (b) Stress changes in materials under pressure

In Fig. 4, in the material SA of the program, the test results of the software were basically consistent with the actual results curve, and the stress and strain changes of the material were within a specific range. The software calculation results for the material were consistent with the actual results, indicating that determining the parameters of the material through the program could better simulate the current damage situation of the material. The peak value and strength were basically consistent under compression and tension. This also indicated that

the program could remind of material damage and stiffness degradation. The curve changes obtained from cyclic loading parameters were consistent with the actual results. To analyze the stress loading analysis results of the current software on materials, the compression analysis diagram in Fig. 5 was obtained by analyzing the compression conditions of different materials.

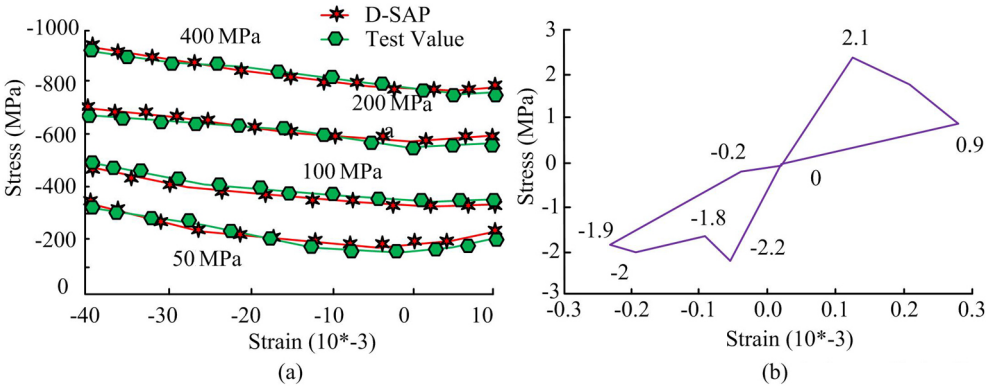

Fig. 5. Stress variation of materials under different compression and cyclic loading: (a) Stress variation curve under high pressure, (b) Stress variation curve during cyclic loading

Fig. 5(a) shows the stress curve changes of the damaged material under different pressures, with pressures of 400 MPa, 200 MPa, 100 MPa, and 50 MPa. The stress variation curves of these four high pressures all varied from large to small. The maximum value of stress under 400 MPa pressure was –800 MPa, –600 MPa under 200 MPa, –390 MPa under 100 MPa, and –170 MPa under 50 MPa. The strain force magnitude and experimental value curve of the material under four different pressure intensities were basically consistent. In Fig. 5(b), after calculation, there was no damage in the state of the material when the stress was between 0 and 1. When the stress exceeded this range, there were plastic changes and damage in the material properties. It may be due to the increase in elastic range of the material in the 0–1 stress range. Through the cyclic pressurization of materials, software can be used to determine the damage and SA of the materials. To test the effectiveness of the software, a displacement comparison was conducted between the material cross-section test units of D-SAP software and composite multi-scale modeling and simulation software (Digima), and Table 1 was obtained.

As shown in Table 1, when analyzing the testing effect of the software, it is found that compared with the real testing results, the material testing results of D-SAP software are significantly better than that of Digimat software, with the smallest deviation value of its system being 0, and the relative deviation value of Digimat software being 0.17%, which indicates that the software is basically able to perfectly replicate and simulate the information parameters of the material when conducting the testing. For all the nodes in Cell 1 and Cell 2, the relative deviation values of D-SAP range from 0% to a maximum of 0.04%, while the relative deviation values of Digimat are in a wider range of 0.016% to 7.5%. This indicates that D-SAP has better stability and accuracy in the simulation process than Digimat software.The relative deviation values of Digimat software are significantly higher than that of D-SAP in nodes 3 and 4 of cell 1.

Table 1. Displacement changes of section test units for two software

Unit No.	Node number	Actual value (m)	Digimat (m)	D-SAP (m)	Relative deviation value of ABAQUS (%)	D-SAP relative deviation value (%)
1	1	$-3.00 \cdot 10^{-4}$	$-3.0051 \cdot 10^{-4}$	$-3.0000 \cdot 10^{-4}$	0.170	0.000
	2	$-3.00 \cdot 10^{-4}$	$-3.0005 \cdot 10^{-4}$	$-3.0001 \cdot 10^{-4}$	0.016	0.003
	3	$-3.50 \cdot 10^{-4}$	$-3.76540 \cdot 10^{-4}$	$-3.5001 \cdot 10^{-4}$	7.500	0.000
	4	$-3.50 \cdot 10^{-4}$	$-3.72560 \cdot 10^{-4}$	$-3.5012 \cdot 10^{-4}$	6.400	0.034
2	1	$-3.00 \cdot 10^{-4}$	$-3.00540 \cdot 10^{-4}$	$-3.0002 \cdot 10^{-4}$	0.180	0.006
	2	$-3.00 \cdot 10^{-4}$	$-3.00870 \cdot 10^{-4}$	$-3.0003 \cdot 10^{-4}$	0.290	0.009
	3	$-3.50 \cdot 10^{-4}$	$-3.68900 \cdot 10^{-4}$	$-3.5004 \cdot 10^{-4}$	5.400	0.012
	4	$-3.50 \cdot 10^{-4}$	$-3.54800 \cdot 10^{-4}$	$-3.5014 \cdot 10^{-4}$	1.600	0.040

This indicates that Digimat has greater limitations in simulating complex materials. To compare the testing and simulation effects of different software on the stress and strain of materials, the above software was combined with the research software for stress-strain testing. Fig. 6 shows the comparison results when selecting 200 MPa and 100 MPa for the applied pressure.

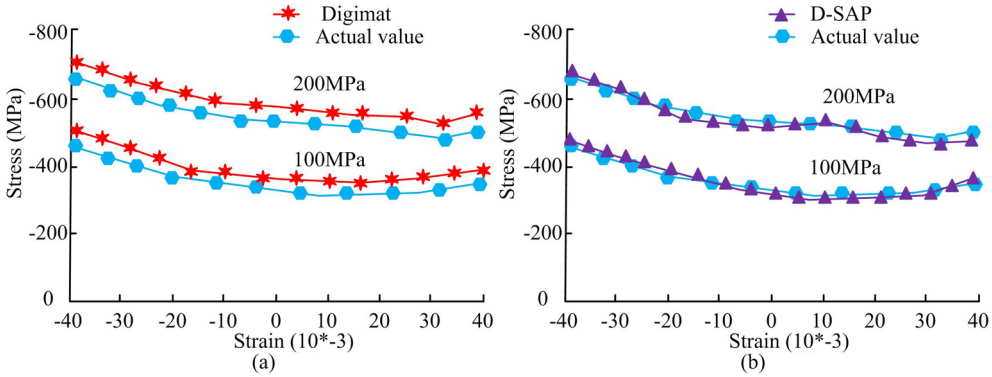

Fig. 6. Comparative testing and analysis of stress and strain between two types of software: (a) Digimat, (b) D-SAP

In Fig. 6, in the stress and strain comparison tests of the two software, the test results of Digimat were slightly lower than the actual test results. Therefore, when using Digit for stress testing of materials, the results of material performance parameters obtained were poor. When conducting stress testing on D-SAP, its stress variation curve was basically the same as the actual test curve. Therefore, D-SAP performs well in testing the stress of materials and could basically fully simulate the stress situation of materials.

5. Conclusions

This study mainly focuses on the analysis of the damage stress effect of plastic materials. D-SAP and finite element unit are used to analyze the damage stiffness and stress changes of plastic materials, and an analysis system based on D-SAP is built. Then, the stress test results of the software are analyzed to test the simulation effect of the current software. The research results indicate that when comparing the performance of D-SAP and Digit in material SA testing, D-SAP performs better in simulating material damage, stress changes, and stiffness degradation. Its test results are close to reality, especially in terms of stress deviation from test values. And D-SAP can achieve a minimum stress change of 0% and a maximum deviation of 1.5% during testing. In multi-axis pressure testing, D-SAP is basically consistent with the test values. Therefore, D-SAP can better simulate the testing of material performance parameters in stress testing of materials. And it can better test, simulate and analyze plastic damaged materials. Although some achievements have been made in this study, there are still some shortcomings. For example, more plastic materials should be selected for analysis when testing materials, and more parameter conditions should be considered for analysis in software testing and analysis. Therefore, more materials and conditions will be selected for analysis and testing in the future.

References

[1] C. Cheng, W. Pan, Y. Huang, and Z. Niu, "Influence of geometry and material on the stress intensity of an interfacial crack propagating from a bi-material notch", *Engineering Analysis with Boundary Elements*, vol. 111, no. 10, pp. 206–211, 2020, doi: 10.1016/j.enganabound.2019.10.016.

[2] T. Bhattacharyya, A.R. Jacob, G. Petekidis, and Y.M. Joshi, "On the nature of flow curve and categorization of thixotropic yield stress materials", *Journal of Rheology*, vol. 67, no. 2, pp. 461–477, 2023, doi: 10.1122/8.0000558.

[3] Y.J. Song, M.D. Yi, G.Q. Zhang, et al., "Design and synthesis of a novel ceramic coating-like tool material", *Ceramics International*, vol. 47, no. 3, pp. 4206–4216, 2020, doi: 10.1016/j.ceramint.2020.09.299.

[4] R.M. Aspden, "Fibre stress and strain in fibre-reinforced composites", *Journal of Materials Science*, vol. 29, pp. 1310–1318, 1994, doi: 10.1007/BF00975081.

[5] Y. Zhou, G. Wu, S. Wang, B. Huang, F.S. Wang, and Z. Wang, "Thermal stress performance of glazed units contained phase change material", *Energy Exploration and Exploitation*, vol. 39, no. 6, pp. 1973–1992, 2021, doi: 10.1177/01445987211015366.

[6] F. Auricchio, E. Bonetti, M. Carraturo, D. Hoemberg, A. Reali, and E. Rocca, "A phase-field based graded-material topology optimization with stress constraint", *Mathematical Models and Methods in Applied Sciences*, vol. 30, no. 8, pp. 1461–1483, 2020, doi: 10.1142/S0218202520500281.

[7] A. Kumar, R. Ghosh, and R. Kumar, "Effects of interfacial crack and implant material on mixed-mode stress intensity factor and prediction of interface failure of cemented acetabular cup", *Journal of Biomedical Materials Research Part B: Applied Biomaterials*, vol. 108, no. 5, pp. 1844–1856, 2020, doi: 10.1002/jbm.b.34526.

[8] A.A. Oyeniran and D.S. Aziaka, "Residual stress consideration in fatigue damage of offshore wind turbine monopiles: To be or not to be?", *World Journal of Mechanics*, vol. 10, no. 4, pp. 39–52, 2020, doi: 10.4236/wjm.2020.104004.

[9] J. Chen, Y.W. Wang, R.Y. Zheng, and X.F. Li, "Mode-III interface crack in a bi-material with initial stress and couple stress", *Engineering Fracture Mechanics*, vol. 281, no. 2, pp. 1–20, 2023, doi: 10.1016/j.engfracmech.2023.109135.

[10] I.R. Siqueira, M. Pasquali, and P.R.D.S. Mendes, "Couette flows of a thixotropic yield-stress material: Performance of a novel fluidity-based constitutive model", *Journal of Rheology*, vol. 64, no. 4, pp. 889–898, 2020, doi: 10.1122/8.0000041.

[11] J. Chen, W. Yao, and D. Gao, “Fatigue life evaluation of tension-compression asymmetric material using local stress–strain method", *Fatigue & Fracture of Engineering Materials & Structures*, vol. 43, no. 9, no. 1994-2005, 2020, doi: 10.1111/ffe.13279.

[12] H.F. Li, S.P. Yang, P. Zhang, Y.Q. Liu, B. Wang, and Z.F. Zhang, “Material-independent stress ratio effect on the fatigue crack growth behavior”, *Engineering Fracture Mechanics*, vol. 259, no. 1, pp. 10–20, 2022, doi: 10.1016/j.engfracmech.2021.108116.

[13] X. Wang, Q. Meng, and W. Hu, “Numerical analysis of low cycle fatigue for welded joints considering welding residual stress and plastic damage under combined bending and local compressive loads”, *Fatigue & Fracture of Engineering Materials & Structures*, vol. 43, no. 5, pp. 1064–1080, 2020, doi: 10.1111/ffe.13216.

[14] H. Matsuoka, T. Otani, and S. Fukui, “Stress distributions in an elastic body due to molecular interactions considering one-dimensional periodic material distribution based on Mindlin’s solution”, *Microsystem Technologies*, vol. 26, no. 1, pp. 139–156, 2020, doi: 10.1007/s00542-019-04537-6.

[15] L. Hassini, “3D model simulating the hydro-mechanical state of unsaturated and deformable material during hot air drying”, *Hydraulic Science and Ocean Engineering*, vol. 2, no. 1, pp. 27–32, 2020, doi: 10.30564/hsme.v2i1.1598.

[16] S. Tu, X. Ren, J. He, and Z. Zhang, “Stress-strain curves of metallic materials and post-necking strain hardening characterization: A review", *Fatigue & Fracture of Engineering Materials & Structures*, vol. 43, no. 1, pp. 3–19, 2020, doi: 10.1111/ffe.13134.

[17] D.S. Stewart and K. Lee, “Modeling the thermcmechanicalhemical behavior of condensed phase reactive materials”, *Propellants Explosives Pyrotechnics*, vol. 45, no. 2, pp. 270–283, 2020, doi: 10.1002/prep.201900221.

[18] H. Kang, P. He, C. Zhang, D. Ying, H. Lv, M. Zhang, and D. Yang, “Stress-strain and burst failure analysis of fiber wound composite material high-pressure vessel”, *Polymers and Polymer Composites*, vol. 29, no. 8, pp. 1291–1303, 2021, doi: 10.1177/0967391120965387.

[19] A.V. Pyatigorets and S.G. Mogilevskaya, “Evaluation of effective transverse mechanical properties of transversely isotropic viscoelastic composite materials”, *Journal of Composite Materials*, vol. 45, no. 25, pp. 2641–2658, 2011, doi: 10.1177/0021998311401091.

[20] M. Goldyn, “Application of the critical shear crack theory for calculation of the punching shear capacity of lightweight aggregate concrete slabs”, *Archives of Civil Engineering*, vol. 69, no. 1, pp. 55–70, 2023, doi: 10.24425/ace.2023.144159.

[21] H. Cui, J. Xia, L. Wu, and M. Xiao, “Reinforcement layout design of three-dimensional members under a state of complex stress”, *Archives of Civil Engineering*, vol. 69, no. 1, pp. 421–436, 2023, doi: 10.24425/ace.2023.144181.

Received: 2024-01-26, Revised: 2024-03-26